ARTICLE

Acidification and Assembly of Porphyrin at an Interface: Counterion Matching, Selectivity, and Supramolecular Chirality

Yiqun Zhang, Penglei Chen,* Yanping Ma, Shenggui He, and Minghua Liu*

Beijing National Laboratory for Molecular Science, Institute of Chemistry, Chinese Academy of Sciences, Beijing 100190, China

ABSTRACT The interfacial diprotonation and assemblies of a free-base achiral porphyrin, 5,10,15,20-tetrakis(3,5-dimethoxyphenyl)-21*H*,23*H*-porphine, on various acidic subphases were investigated. It has been shown that the compound could be diprotonated in situ on an acidic subphase and can form assemblies. The interfacially organized supramolecular assemblies were transferred onto a solid substrate, and the assemblies showed supramolecular chirality. Interestingly, the supramolecular chirality of the assemblies of the diprotonated species showed a counterion-dependent behavior. For the assemblies fabricated from the aqueous HCl subphases, a strong Cotton effect (CE) could be observed, although the porphyrin itself is achiral. When an aqueous HBr solution was used as the subphase, the assemblies showed a weak CE, whereas no CE could be detected for the assemblies formulated from the HNO_3 or HI subphase. Interestingly, when a mixture of HBr and NaCl, or HNO_3 and NaCl, was employed as the subphase, the formed assemblies displayed chiral features similar to those fabricated on the HCl subphase, suggesting that the Cl^- could be preferentially visualized in terms of supramolecular chirality, although the system itself is composed of achiral species. On the basis of the experimental facts and a theoretical calculation, an explanation with regard to the different sizes of the counterions and the distinct binding affinities of the counteranions to the diprotonated porphyrin species has been proposed. Our findings provide new insights into the assembly of the diprotonated porphyrins as well as the interfacially occurring symmetry breaking.

KEYWORDS: porphyrinoids • diprotonation • counterion • interfacial assembly • supramolecular chirality • symmetry breaking

INTRODUCTION

Porphyrinoids, which are composed of four pyrrole rings bridged together via the α position through four methine groups, are multifunctional organic dyes showing distinct chemical versatility and excellent biological compatibility (1−3). Their unique planar as well as rigid molecular geometry and aromatic electronic feature delocalized over the molecular frame enable them to possess peculiar and tunable spectroscopic, photophysical, photochemical, and assembly properties (2). By virtue of these excellent features, porphyrins have received much attention as ideal building blocks for the construction of noncovalent supramolecular assemblies with motivations for potential applications in photoelectronic and nonlinear optical devices, information storage and transfer, and light energy conversion, and as an nice model for the investigation of energy, electron, charge, and ion transportation in the naturally occurring light-harvesting antenna complexes and the photosynthetic reaction centers (2, 3). To date, a wide variety of organized supramolecular assemblies containing porphyrin units have been developed and investigated intensively (2−6).

On the other hand, it is also an interesting issue endowing porphyrin-involved molecular assemblies with chirality, which is applicable to a wide range of fields including smart soft nanomaterials for data storage and processing, chiral sensing, optobioelectronics, chiroptical devices, catalysis, biochemistry, and so forth (7). Porphyrin units have been considered to be one of the most useful building blocks that connect supramolecular chemistry and chiral chemistry (7−15). Besides the intrinsically chiral porphyrin species (8, 9), achiral analogues could also be organized to form chiral superstructures by (i) assembling in a chiral circumstance, where a chiral species or template works as a chirality inducer (10−12), or (ii) assembling in a directional stirring solution, through a directional spinning coating, or by the interfacial organization (13, 14). The latter scenario has, in particular, gained great attention because it might be related to the origin of chirality in nature and the mirror-symmetry breaking of a system (13, 14, 16).

For a free-base porphyrin, its central nitrogen atoms can be diprotonated by strong acids, where two counteranions are attached in the axial position in a near-symmetrical manner above and below the porphyrin macrocycle (17). From this point of view, the assembly of porphyrins can be generally divided into two categories: one is the assembly of conventional porphyrins without axial ligands; the other is the diprotonated species. For the latter case, the axially attached counterions would significantly affect their assembly properties. The aggregation behaviors of the diprotonated porphyrins with charged (18) or neutral (17a, 19) groups in the periphery have recently been intensively studied in terms of the role of the counterions. While there

* Corresponding authors. Tel: (+) 86-10-82612655. Fax: (+) 86-10-62569564. E-mail: chenpl@iccas.ac.cn (P.C.), liumh@iccas.ac.cn (M.L.).
Received for review June 9, 2009 and accepted August 17, 2009

DOI: 10.1021/am900399w

Published on Web 09/02/2009

Scheme 1. Illustration of Counterion Matching, Selectivity, and Supramolecular Chirality[a]

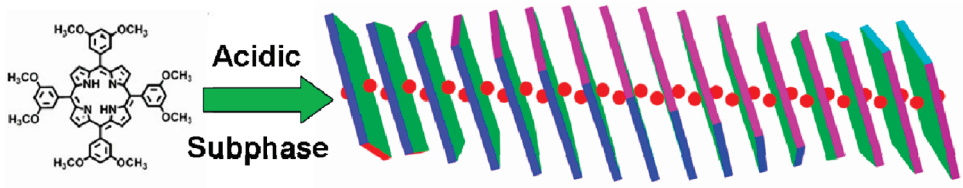

[a] Although the diprotonated porphyrins are distorted, they are abbreviated as the plate for clarity. The red balls represent the axially bonded counterions.

are a lot of investigations on the supramolecular assembly of free-base porphyrins and on the assembly behavior of the diprotonated porphyrins (17a, 18–20), there are fewer reports on the supramolecular chirality of the diprotonated porphyrins (13a–13d) substituted with neutral groups in terms of the effects of counterions.

In this paper, we report the assembly of a diprotonated porphyrin through interfacial organization. We have found that an achiral porphyrin, 5,10,15,20-tetrakis(3,5-dimethoxyphenyl)-21*H*,23*H*-porphine (H_2TPPDOMe; Scheme 1), could be diprotonated and fabricated into various aggregates on aqueous HX (X = Cl^-, Br^-, I^-, and NO_3^-) subphases. We have further found that the formed assemblies show supramolecular chirality (14, 21), which is currently an important topic in porphyrin assemblies (7–15). Interestingly, the supramolecular chirality of the diprotonated porphyrin displayed a counterion matching effect. That is, when the diprotonated species are axially separated through Cl^-, the porphyrin assemblies show strong bisignated circular dichroism (CD) signals. When Br^- is used, the assemblies show weak monosignated CD signals. When I^- or NO_3^- is used, no CD signal could be detected. More interestingly, Cl^- could be predominantly incorporated into the neighboring diprotonated species, resulting in the formation of chiral assemblies, even when the molar concentration of Cl^- in the subphase is only 0.8% NO_3^- or 4% Br^-. To the best of our knowledge, this is the first report that relates the supramolecular chirality of the diprotonated porphyrin assemblies to the counterions. These findings provide new insights into the assembly of the diprotonated porphyrins and the interfacially occurring symmetry breaking.

EXPERIMENTAL SECTION

Materials. The achiral porphyrin derivative, 5,10,15,20-tetrakis(3,5-dimethoxyphenyl)-21*H*,23*H*-porphine (H_2TPPDOMe, TCI, 95%), was used as received without further purification. Concentrated hydrochloric acid (HCl), a hydrobromic acid subphase (HBr), a hydriodic acid subphase (HI), and nitric acid (HNO_3) were purchased from Beijing Yili Fine Chemical Co., Ltd. HCl was diluted to 2.4 M, and the other acids were diluted to 1.2 M before use as the subphase (22).

Procedures and Methods. The floating films on various aqueous HX acid subphases were produced by spreading chloroform solutions of H_2TPPDOMe (5×10^{-5} mol/L) onto the corresponding subphases. Surface pressure–molecular area (π–A) isotherms in each case were recorded by using a KSV (KSV 1100) instrument with a compressing speed of 7.5 cm^2/min after a delay of 20 min while the chloroform solvent evaporated. For film deposition, the floating films were compressed with a speed of 7.5 cm^2/min to 30 mN/m, at which the compressed films were transferred onto the required solid supports by a horizontal lifting method using the KSV 1100 LB apparatus. The size of the solid substrates was ca. 0.5 cm × 1.2 cm. The transfer ratio in all of the cases is close to 1. Hydrophobic quartz slides were achieved by immersion of the clean slides in a solution of octadecyltrichlorosilane. The hydrophobic quartz slides were then used as the solid supports for UV–vis, CD, and linear dichroism (LD) spectral measurements. For atomic force microscopy (AFM) and X-ray photoelectron spectroscopy (XPS) investigations, hydrophobic single-face-polished silicon wafers were employed as solid supports. The fabricated samples were then subjected to various measurements. In order to obtain acidified chloroform solutions of the compound, a glass capillary was kept in the corresponding aqueous HX acid solutions for about 2 min; then the glass capillary was drawn out and immediately immersed in 1 mL of the newly confected chloroform solutions of H_2TPPDOMe. Generally, about 10–15 μL of concentrated HX acids was added to 800 μL of a chloroform solution (5×10^{-5} M) to achieve a diprotonated species, which gave a stable solution. After 1 min under magnetic stirring, the solutions were subjected to UV–vis and CD spectral measurements.

Theoretical Calculation. A theoretical calculation on the structures of the diprotonated H_2TPPDOMe species was carried out using the *Gaussian 03* package with density functional theory at the PBE1PBE/6-311G* level.

Apparatus and Measurements. Jasco UV-550 and J-815 CD spectropolarimeters were employed for the UV–vis, CD, and LD spectral measurements, respectively. In the measurement of the CD and LD spectra, the sample was placed perpendicularly to the light path and at the same time was rotated continuously within the film plane by a homemade rotator, in order to eliminate the LD and linear birefringence (LB) artifacts and to obtain the LB- and LD-free CD spectra (14, 21, 23). The AFM height images without any image processing except flattening were recorded on a Digital Instrument Nanoscope IIIa Multimode system (Santa Barbara, CA) with a silicon cantilever using the tapping mode. The XPS data were obtained with an ESCALab220i-XL electron spectrometer from VG Scientific using 300 W Mg Kα radiation. The base pressure was about 3×10^{-9} mbar. The binding energies were referenced to the C 1s line at 284.9 eV from adventitious carbon.

RESULTS AND DISCUSSION

π–A Isotherms of the H_2TPPDOMe Films Formed on Various Aqueous HX Acid Surfaces. Figure 1 shows the π–A isotherms of the films of H_2TPPDOMe formed on various aqueous HX acid surfaces. The limiting areas per molecule deduced by extrapolating the steepest rising part of the π–A curves are 0.92, 1.23, 1.08, and 1.30 nm^2 for the film floating on HCl, HBr, HI, and HNO_3 subphases, respectively. These values are larger than that of the film floating on a pure Milli-Q water surface (0.70 nm^2), suggesting that the counterions might be inserted in the molecular assemblies (14a). These values show an

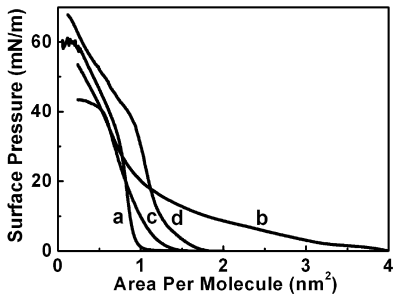

FIGURE 1. $\pi-A$ **isotherms of H_2TPPDOMe on HCl (a), HBr (b), HI (c), and HNO_3 (d) subphases at 20 °C.**

increasing tendency in the order of Cl^-, Br^-, and NO_3^-, whereas in the case of I^-, this value does not follow this tendency. One possible reason for this is that the diprotonated species might form a multilayer or aggregates rather than a monolayer because of the lack of long alkyl chains. Similar phenomena have been observed from other molecules that bear very short or no alkyl chains (24).

UV−Vis Spectra of the Assemblies of H_2TPPDOMe Formed on Various Aqueous HX Acid Surfaces. Experimentally, the chloroform solution of H_2TPPDOMe was spread onto various aqueous HX subphases (22), and the Langmuir−Schaefer (LS) (25) films were fabricated at 30 mN/m. The UV−vis spectra of the assemblies formed on diverse aqueous HX acid subphases are presented in Figure 2 and summarized in Table 1. As shown in Figure 2a, a Soret band maximum at 422 nm and four Q bands in the region of 490−670 nm are observed for the chloroform solution of the compound. Upon acidification in a chloroform solution by HCl, a bathochromic-shifted Soret band appears at 458 nm, and two Q bands appear at 607 and 660 nm, suggesting diprotonation of the central nitrogen atoms of H_2TPPDOMe (14a, 17b, 19d). As a result, $[H_4TPPDOMe]Cl_2$ species are formed in the chloroform solution of the compound. Similar results were observed when the chloroform solution was acidified by HBr, HI, and HNO_3, indicating the formation of the corresponding diprotonated $[H_4TPPDOMe]X_2$ ($X = Br^-$, I^-, and NO_3^-) species in solutions.

It is suggested based on the exciton coupling model proposed by Kasha and co-workers (26) that the Soret band of the J aggregates of a porphyrin chromophore is split into two bands (27). The narrowed band, which is parallel to the aggregate axis, displays bathochromic shifts compared with that of the monomer, while the broad one, which is perpendicular to the aggregate axis, displays hypsochromic shifts. In the case of the H aggregates, a blue-shifted Soret band could be observed (26, 27). In the present cases, for the assemblies deposited from aqueous HCl subphases, a Soret band maximum at 427 nm and two Q bands at 626 and 672 nm are detected, suggesting that $[H_4TPPDOMe]Cl_2$ species are in situ formed on the surface of an aqueous HCl subphase (14a, 17b, 19d). The maximum absorption of the Soret band shows a hypsochromic shift with respect to that of the HCl-acidified chloroform solution. Also, it is broadened compared with that of the monomeric diprotonated species in solution. These results suggest that most of the $[H_4TPPDOMe]Cl_2$ species are mainly arranged as various nonspecific H-type aggregates in the transferred film, where some nonspecific J-type aggregates might also exist (14a, 26, 28).

When the porphyrin is spread on the aqueous subphase of HBr and HI, two rather than four Q bands are detected from the deposited films, suggesting the in situ formation of $[H_4TPPDOMe]X_2$ ($X = Br^-$ and I^-) species on the corresponding aqueous HX subphases. At the same time, the maximum absorption of the Soret band of the formed assemblies displays bathochromic shifts and becomes broadened compared with those of the chloroform solutions acidified by HBr and HI, respectively. Also, the broadened Soret bands show no distinct split, which might be due to the superposition of various aggregates. These facts indicate that $[H_4TPPDOMe]X_2$ species mainly form various nonspecific J-type aggregates accompanied by some nonspecific H-type aggregates when other counteranions such as Br^- and I^- are employed (14a, 26, 28). When HNO_3 is employed as the subphase, the UV−vis spectrum of the transferred film displays features similar to those observed from the films deposited from HBr and HI subphases except that a weak Q band at ca. 601 nm (a Q band displayed by the monomeric $[H_4TPPDOMe](NO_3)_2$ species in solution) is also observed. This indicates that, besides various nonspecific J- and H-type aggregates, there might also be some monomeric $[H_4TPPDOMe](NO_3)_2$ species in the deposited film. These results indicate that the counterions have significant effects on the interfacial assemblies of the diprotonated porphyrins.

CD Spectra of the Assemblies of H_2TPPDOMe Formed on Various Aqueous HX Acid Surfaces. As summarized in Table 1 and shown in Figure 2, all of the HX-acidified chloroform solutions of H_2TPPDOMe are CD-silent. However, as shown in Figure 2a, the films deposited from an aqueous HCl surface display strong bisignated Cotton effect (CE) maxima at 397 and 445 nm, with one crossover at 414 nm, and a monosignated CE maximum at 669 nm, which corresponds to the Soret and Q bands of $[H_4TPPDOMe]Cl_2$ species in the films, respectively (14a). The CD signals could be opposite for the films deposited from the different batches, suggesting that the observed chirality of the films was formed through a spontaneous symmetry breaking rather than from any chiral impurities. This phenomenon is essentially the same as that reported for the chirality of the assemblies obtained from achiral species, in which achiral units were cooperatively stacked in a helical-sense conformation (13a−13d, 14, 21, 29). When an aqueous HBr solution is used as the subphase (Figure 2b), the fabricated film shows rather weak monosignated CE at 475 nm in the Soret band and at 694 nm in the Q band. In contrast, all of the films deposited from an aqueous HI or HNO_3 solution are CD-silent, as presented in Figure 2c,d.

Moreover, in order to validate the authenticity of the observed CD spectra. The LD spectra of the films had also been investigated. A comparison of the CD and LD spectra measured from a film of the compound deposited from an aqueous HCl acid surface was carried out. On the basis of a semiempirical equation (13f, 30), the contribution of the LD

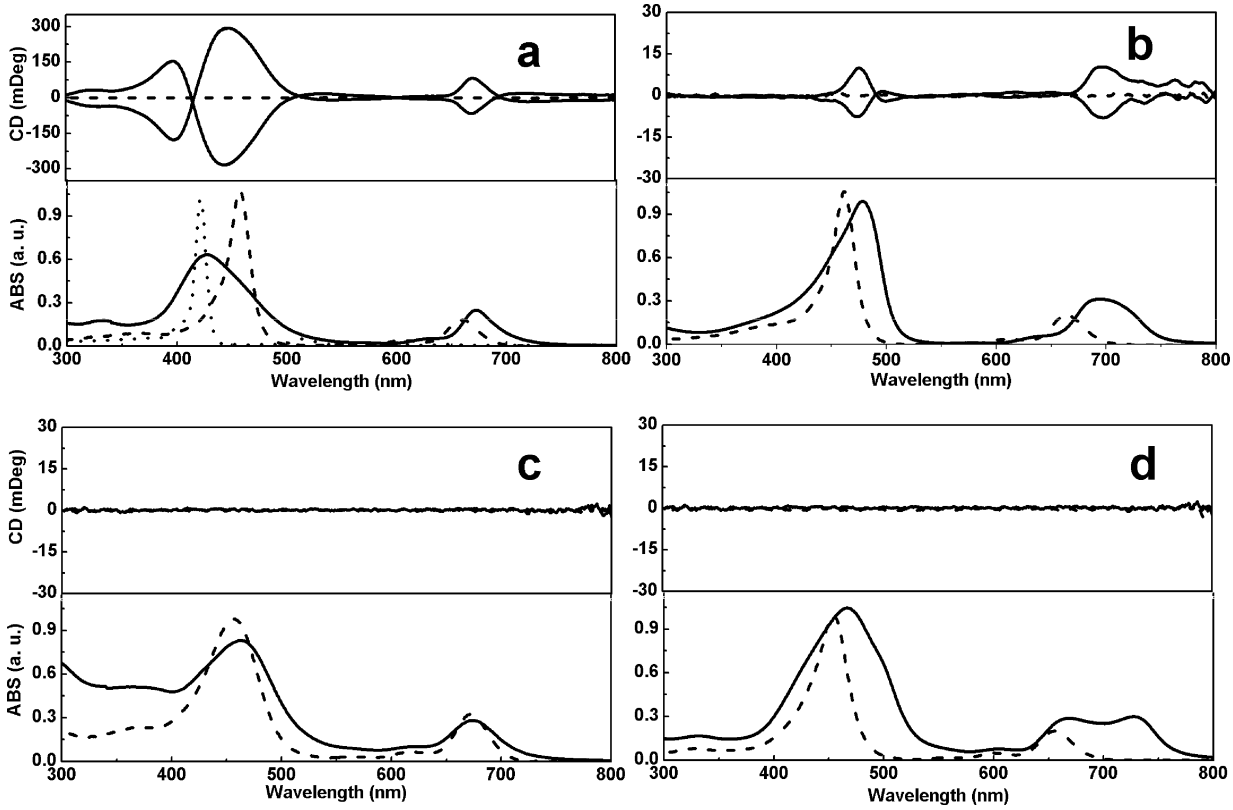

FIGURE 2. (a) UV−vis (bottom panel) spectra of H_2TPPDOMe in a chloroform solution (dotted line), in a HCl-acidified chloroform solution (dashed line), and in LS films deposited from aqueous HCl subphases (solid line) and the CD spectra (top panel) of the compound in a HCl-acidified chloroform solution (dashed line) and in the LS films deposited from aqueous HCl subphases (solid line). The two solid CD curves were obtained from the films deposited in different batches. The corresponding HX acids are aqueous HBr (b), HI (c), and HNO_3 (d) solutions, respectively. All of the films were deposited at 30 mN/m.

Table 1. Absorption Maximum in UV−Vis and CD Spectra of Various Solutions and LS Films

	UV−vis spectra (nm)		CE maxima (nm)	
sample	Soret band	Q band	Soret band	Q band
chloroform solution	422	516, 550, 589, 648		
HCl-acidified $CHCl_3$ solution	458	607, 660		
HBr-acidified $CHCl_3$ solution	462	613, 665		
HI-acidified $CHCl_3$ solution	457	619, 673		
HNO_3-acidified $CHCl_3$ solution	454	601, 656		
LS film (2.4 M HCl subphase)	427	626, 672	397, 445	669
LS film (1.2 M HBr subphase)	479	635, 695	475	694
LS film (1.2 M HI subphase)	463	619, 674		
LS film (1.2 M HNO_3 subphase)	467	601, 669, 727		
LS film (1.2 M HNO_3/2 mM NaCl)	466	664, 727		
LS film (1.2 M HNO_3/ 5 mM NaCl)	462	672, 724	420, 444	667
LS film (1.2 M HNO_3/10 mM NaCl)	428	627, 672	402, 452	667
LS film (1.2 M HBr/10 mM NaCl)	479	640, 701	467, 487	706
LS film (1.2 M HBr/ 50 mM NaCl)	438	631, 674	406, 462	678

artifact to the CD spectra could be estimated to be ca. 4.3%. This confirms that the detected CD spectra do not result from the macroscopic anisotropy of the deposited film but from the intrinsic chiral feature of the supramolecular assemblies.

AFM Images of the Assemblies Formed on Various Aqueous HX Acid Surfaces. Additionally, when the AFM images of the films deposited from these acidic subphases were measured, nanofibers were observed for the films deposited from an aqueous HCl (14a) or HBr subphase, while nanoparticles were detected when an aqueous HI or HNO_3 solution was used (Figure 3). The nanofibers formed on HCl and HBr subphases are ca. 4.5 and 3.7 nm in height and ca. 40 and 50 nm in width, respectively. The nanoparticles formed on HI and HNO_3 surfaces are ca. 10 and 25 nm in height and ca. 100 and 150 nm in width, respectively. The formation of these nanostructures seems to be related to the counterion in the assemblies. Larger counterions favor the formation of nanoparticles, while small counterions prefer the nanofiber structure. In addition, the nanostructures do not cover the whole area of the surface.

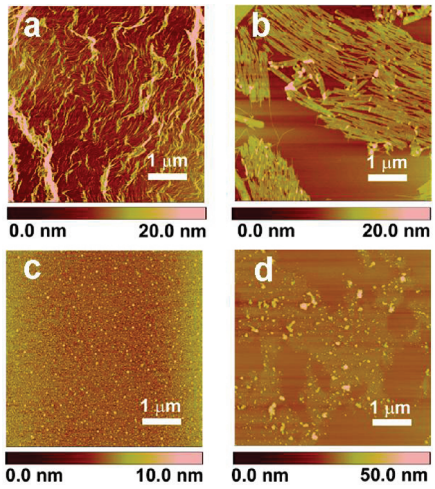

FIGURE 3. AFM images of the films of H_2TPPDOMe deposited from HCl (a), HBr (b), HI (c), and HNO_3 (d) surfaces at 30 mN/m. Image size: 5 μm × 5 μm for all of the cases.

These results confirm that the diprotonated species formed multilayer or aggregates rather than monolayer films at the air/water interface, which is in agreement with the π–A isotherms.

As described in the above paragraphs, although the diprotonated species themselves are achiral, CD absorptions could be detected from the nanofibers formed on HCl and HBr subphases. These results are basically the same as those reported for our previous systems, where CD signals as well as helical or spiral structures, or straight nanofibers, were obtained for the films fabricated from achiral amphiphiles through interfacial organization (14, 21). The macroscopic supramolecular chirality in these films has been suggested to be caused by the predominant one-handedness, helical sense stacking of the building blocks during lateral compression of the floating films.

Preferential Visualization of Cl^- in Terms of Supramolecular Chirality. Interestingly, the diprotonated species further displays a preferential selectivity for Cl^-. When we spread the porphyrin on the subphase of an aqueous HNO_3 or HBr solution in the presence of Cl^-, we found that Cl^- was predominantly incorporated into the assemblies. Figure 4a shows the CD and UV–vis spectra of the films deposited from an aqueous HNO_3 + NaCl subphase. When 0.002 M NaCl coexists with 1.2 M HNO_3, the fabricated film displays a broad Soret band at 466 nm and the film is almost CD-silent. However, when 0.005 M NaCl is contained in the 1.2 M HNO_3 solution, a blue-shifted shoulder peak at 430 nm around the Soret band is observed from the UV–vis spectrum and a weak CE around this shoulder peak was detected. When the concentration of NaCl increased to 0.01 M, the UV–vis spectrum of the film exhibits a broadened Soret band at 428 nm and two Q bands at 627 and 672 nm, the profile of which is rather similar to those of the films fabricated from aqueous HCl subphase. Moreover, the CD spectrum of the film displays strong bisignated and monosignated CE values around the Soret and Q bands, respectively, whose profiles are almost the same as those of the film deposited from an aqueous HCl subphase. When HBr + NaCl is employed as the subphase, similar results are observed, as shown in Figure 4b.

Because the film fabricated from an aqueous HBr surface shows weak monosignated CE and that from an aqueous HNO_3 surface shows no CD signal, the present results suggest that Cl^- is selectively incorporated into the assemblies when spreading on a subphase containing a Cl^- ion, although the molar ratio of Cl^- is only 0.8% NO_3^-. In order to confirm this, we measured the XPS spectra of the film deposited from the aqueous subphase of HNO_3 + NaCl, as shown in Figure 5. It can be seen that, although the molar concentration of Cl^- in the subphase was only 0.8% NO_3^-, the XPS of the film deposited from this subphase displayed distinct binding energies at 198.3 eV (Cl 2p) and 400.2 eV (N 1s; nitrogen atoms of porphyrin), whereas the binding energy of the nitrogen atom of NO_3^-, which should be at 406.2 eV, is negligible.

Optimized Molecular Structure of the $[H_4TPPDOMe]X_2$ Species on the Basis of a Theoretical Calculation. In order to further survey the mechanism of the above-described experimental facts, the optimized molecular structures of the $[H_4TPPDOMe]X_2$ species are theoretically calculated. As shown in Figure 6, it can be seen that all of the $[H_4TPPDOMe]X_2$ species have a saddling conformation, where two counteranions are combined in a near-symmetrical manner at the axial position through the hydrogen bonds above and below the mean macrocyclic plane. These results are essentially analogous to those reported by others, where it is believed that the diprotonation of free-base porphyrins could result in a deformation of the porphyrin plane, giving a saddling conformation, where two counteranions are attached at the axial position above and below the mean macrocyclic plane (17). We further found that the distance between the two axially attached counteranions is ca. 4.70, 5.14, 5.80, and 6.98 Å for Cl^-, Br^-, I^-, and NO_3^-, respectively, showing an increasing tendency. Consequently, our present optimized results are substantially the same as those suggested by other researchers, where it is concluded that the distance from the counteranion to the mean macrocyclic plane display an increasing tendency with an increase in the size of the counteranion (31). Thus, we can suggest that the neighboring diprotonated porphyrin species are separated in the order of Cl^-, Br^-, I^-, and NO_3^- ions when our porphyrin is assembled on the corresponding aqueous HX subphases.

Explanation for Counterion Matching, Selectivity, and Supramolecular Chirality. On the basis of our experimental facts and the calculated theoretical models, a reasonable explanation for the interesting counterion matching and selectivity with respect to the supramolecular chirality could be proposed, as shown in Scheme 1. As proven by the UV–vis and CD/LD spectra, when the porphyrin is spread at the air/acid interface, in situ diprotonation occurs and these diprotonated species could possibly show a cooperative stacking in a helical sense, resulting in the formation of chiral supramolecular assemblies (13a–13d,

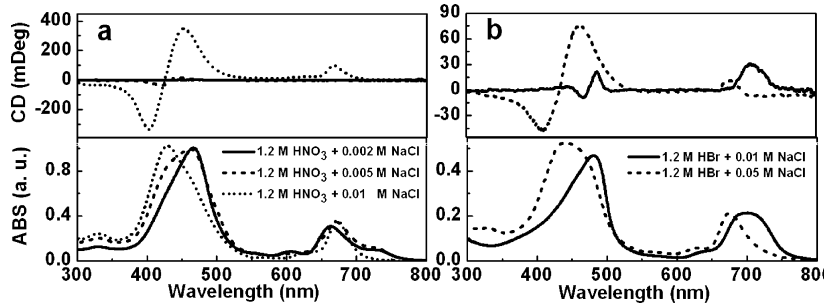

FIGURE 4. CD (top panel) and UV−vis (bottom panel) spectra of the films of H_2TPPDOMe deposited from aqueous HNO_3 + NaCl (a) and HBr + NaCl (b) subphases. All of the films were deposited at 30 mN/m.

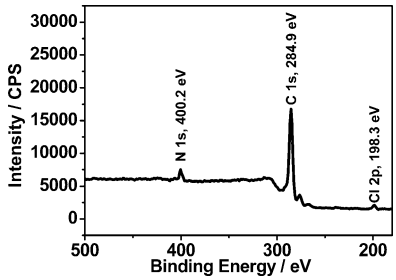

FIGURE 5. XPS spectrum of the film deposited from a 1.2 M HNO_3 + 0.01 M NaCl subphase.

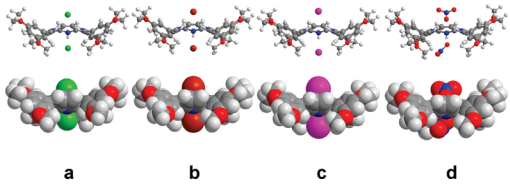

FIGURE 6. Optimized molecular structures of the $[H_4TPPDOMe]X_2$ species, where X = Cl^- (a), Br^- (b), I^- (c), and NO_3^- (d). The ball-and-stick and space-filling models are presented in the upper and lower panels, respectively.

14, 21, 29). Such cooperative packing is related to the $\pi-\pi$ overlapping as well as the separated distance between the neighboring porphyrins (21c, 32). When Cl^- is inserted, the neighboring $[H_4TPPDOMe]Cl_2$ building blocks show the biggest extent of $\pi-\pi$ overlapping and the smallest distance between them because Cl^- has the smallest size and most of the $[H_4TPPDOMe]Cl_2$ units are mainly packed as various H aggregates (26). Thus, we observed a strong exciton couplet in the CD spectra of the assemblies of $[H_4TPPDOMe]Cl_2$. When the anions with bigger size, such as I^- and NO_3^-, are employed, the cooperative stacking of the diprotonated species is prohibited because of the far separation and smaller extent of $\pi-\pi$ overlapping of the neighboring chromophore; thus, no CD signal could be detected.

Comparatively, in the case of counterion Br^-, whose size is bigger than Cl^- but smaller than I^- and NO_3^-, there exists a smaller extent of $\pi-\pi$ overlapping and a larger distance between the $[H_4TPPDOMe]Br_2$ building blocks than between the $[H_4TPPDOMe]Cl_2$ units. Furthermore, there exists a larger extent of $\pi-\pi$ overlapping and a smaller distance between the $[H_4TPPDOMe]Br_2$ building blocks than between the $[H_4TPPDOMe]I_2$ or $[H_4TPPDOMe](NO_3)_2$ units. Therefore, weak monosignated CD signals could be detected from the assemblies formed on an aqueous HBr subphase.

On the other hand, when the porphyrin was assembled on a mixed solution of HNO_3 + NaCl, or HBr + NaCl, Cl^- could be preferentially combined in the molecular assemblies, although its concentration was extremely lower than that of NO_3^- or Br^-. This is due to the higher affinity between Cl^- and the diprotonated porphyrin species than between NO_3^- (Br^-) and the diprotonated porphyrin species (33). Thus, the counterion selectivity in our system is a consequence of the fact that the $[H_4TPPDOMe]Cl_2$ aggregates are more stable than the others. By utilizing this property, we can use the porphyrin assemblies to detect the Cl^- ion in the subphase in terms of supramolecular chirality, although all of the involved species were achiral.

CONCLUSIONS

In summary, we have shown that an achiral free-base porphyrin could be diprotonated in situ on various acidic subphases, and the protonated species could form counterion-dependent assemblies. There exists an ion matching between the supramolecular chirality of the assemblies and Cl^-. That is, when the counterion is Cl^-, a strong exciton couplet could exist in the assemblies, while only weak or even no CD signal could be detected for other counterions. Moreover, the diprotonated species show a predominant selectivity for Cl^- when spreading on a mixed solution of acid and NaCl. These findings provide new insight into the assembly of the diprotonated porphyrin and correlate the assembly structure with their supramolecular chirality.

Acknowledgment. This work was financially supported by the National Natural Science Foundation of China (Grants 20533050, 20773141, and 20873159) and the Fund of the Chinese Academy of Sciences, the National Research Fund for Fundamental Key Project 973 (Grants 2007CB808005 and 2006CB932101).

REFERENCES AND NOTES

(1) (a) Woggon, W.-D. *Acc. Chem. Res.* **2005**, *38*, 127–136. (b) Balaban, T. S. *Acc. Chem. Res.* **2005**, *38*, 612–623. (c) Langa, K.; Mosinger, J.; Wagnerová, D. M. *Coord. Chem. Rev.* **2004**, *248*, 321–350. (d) Sessler, J. L. *J. Porphyrins Phthalocyanines* **2000**, *4*, 331–336.

(2) Scandola, F.; Chiorboli, C.; Prodi, A.; Iengo, E.; Alessio, E. *Coord. Chem. Rev.* **2006**, *250*, 1471–1496.

(3) For reviews, see: (a) Prodi, A.; Indelli, M. T.; Kleverlaan, C. J.; Alessio, E.; Scandola, F. *Coord. Chem. Rev.* **2002**, *229*, 51–58. (b) Imamura, T.; Fukushima, K. *Coord. Chem. Rev.* **2000**, *198*, 133–156. (c) Wojaczyński, J.; Latos-Grażyński, L. *Coord. Chem. Rev.* **2000**, *204*, 113–171. (d) Hoeben, F. J. M.; Jonkheijm, P.; Meijer,

E. W.; Schenning, A. P. H. J. *Chem. Rev.* **2005**, *105*, 1491–1546. (e) You, C.-C.; Dobrawa, R.; Saha-Möler, C. R.; Würthner, F. *Top. Curr. Chem.* **2005**, *258*, 39–82. (f) Elemans, J. A. A. W.; Van Hameren, R.; Nolte, R. J. M.; Rowan, A. E. *Adv. Mater.* **2006**, *18*, 1251–1266. (g) Satake, A.; Kobuke, Y. *Tetrahedron* **2005**, *61*, 13–41. (h) Bouamaied, I.; Coskun, T.; Stulz, E. *Struct. Bonding* **2006**, *121*, 1–47. (i) Choi, M.-S.; Yamazaki, T.; Yamazaki, I.; Aida, T. *Angew. Chem., Int. Ed.* **2004**, *43*, 150–158. (j) Lee, S. J.; Hupp, J. T. *Coord. Chem. Rev.* **2006**, *250*, 1710–1723.

(4) (a) Van Hameren, R.; Schön, P.; Van Buul, A. M.; Hoogboom, J.; Lazarenko, S. V.; Gerritsen, J. W.; Engelkamp, H.; Christianen, P. C. M.; Heus, H. A.; Maan, J. C.; Rasing, T.; Speller, S.; Rowan, A. E.; Elemans, J. A. A. W.; Nolte, R. J. M. *Science* **2006**, *314*, 1433–1436. (b) Elemans, J. A. A.; Lensen, M. C.; Gerritsen, J. W.; Van Kempen, H.; Speller, S.; Nolte, R. J. M.; Rowan, A. E. *Adv. Mater.* **2003**, *15*, 2070–2073. (c) Tsuda, A.; Nakamura, T.; Sakamoto, S.; Yamaguchi, K.; Osuka, A. *Angew. Chem., Int. Ed.* **2002**, *41*, 2817–2821. (d) Youm, K.-T.; Nguyen, S. T.; Hupp, J. T. *Chem. Commun.* **2008**, 3375–3377. (e) Hasobe, T.; Oki, H.; Sandanayakaa, A. S. D.; Murata, H. *Chem. Commun.* **2008**, 724–726. (f) Stang, P. J.; Fan, J.; Olenyuk, B. *Chem. Commun.* **1997**, 1453–1454. (g) Johnston, M. R.; Gunter, M. J.; Warrener, R. N. *Chem. Commun.* **1998**, 2739–2740. (h) Diskin-Posner, Y.; Patra, G. K.; Goldberg, I. *Chem. Commun.* **2002**, 1420–1421 (j).

(5) (a) Kleij, A. W.; Kuil, M.; Tooke, D. M.; Lutz, M.; Spek, A. L.; Reek, J. N. H. *Chem.—Eur. J.* **2005**, *11*, 4743–4750. (b) Otsuki, J.; Iwasaki, K.; Nakano, Y.; Itou, M.; Araki, Y.; Ito, O. *Chem.—Eur. J.* **2004**, *10*, 3461–3466. (c) De Luca, G.; Pollicino, G.; Romeo, A.; Patanè, S.; Scolaro, L. M. *Chem. Mater.* **2006**, *18*, 5429–5436. (d) Prodi, A.; Chiorboli, C.; Scandola, F.; Iengo, E.; Alessio, E.; Dobrawa, R.; Wü rthner, F. *J. Am. Chem. Soc.* **2005**, *127*, 1454–1462. (e) Schenning, A. P. H. J.; Benneker, F. B. G.; Geurts, H. P. M.; Liu, X. Y.; Nolte, R. J. M. *J. Am. Chem. Soc.* **1996**, *118*, 8549–8552. (f) Hwang, I.-W.; Kamada, T.; Ahn, T. K.; Ko, D. M.; Nakamura, T.; Tsuda, A.; Osuka, A.; Kim, D. *J. Am. Chem. Soc.* **2004**, *126*, 16187–16198. (g) Iengo, E.; Zangrando, E.; Minatel, R.; Alessio, E. *J. Am. Chem. Soc.* **2002**, *124*, 1003–1013. (h) Moschetto, G.; Lauceri, R.; Gulino, F. G.; Sciotto, D.; Purrello, R. *J. Am. Chem. Soc.* **2002**, *124*, 14536–14537. (i) Micali, N.; Villari, V.; Castriciano, M. A.; Romeo, A.; Scolaro, L. M. *J. Phys. Chem. B* **2006**, *110*, 8289–8295. (j) Hartnell, R. D.; Arnold, D. P. *Organometallics* **2004**, *23*, 391–399.

(6) (a) Borovkov, V. V.; Lintuluoto, J. M.; Sugeta, H.; Fujiki, M.; Arakawa, R.; Inoue, Y. *J. Am. Chem. Soc.* **2002**, *124*, 2993–3006. (b) Wu, J.-J.; Li, N.; Li, K.-A.; Liu, F. *J. Phys. Chem. B* **2008**, *112*, 8134–8138.

(7) For reviews, see: (a) Borovkov, V. V.; Inoue, Y. *Top. Curr. Chem.* **2006**, *265*, 89–146. (b) Hembury, G. A.; Borovkov, V. V.; Inoue, Y. *Chem. Rev.* **2008**, *108*, 1–73. (c) Rosaria, L.; D'Urso, A.; Mammana, A.; Purrell, R. *Chirality* **2008**, *20*, 411–419. (d) Berova, N.; Di Bari, L.; Pescitelli, G. *Chem. Soc. Rev.* **2007**, *36*, 914–931.

(8) (a) Arai, T.; Takei, K.; Ogawa, Y.; Nishino, N. *Eur. J. Org. Chem.* **2005**, 5067–5076. (b) Maurer, K.; Hager, K.; Hirsch, A. *Eur. J. Org. Chem.* **2006**, *333*, 8–3347. (c) Bouamaied, I.; Fendt, L.-A.; Wiesner, M.; Hässinger, D.; Amiot, N.; Thöi, S.; Stulz, E. *Pure Appl. Chem.* **2006**, *78*, 2003–2014. (d) Balaban, T. S.; Bhise, A. D.; Fischer, M.; Linke-Schaetzel, M.; Roussel, C.; Vanthuyne, N. *Angew. Chem., Int. Ed.* **2003**, *42*, 2140–2144. (e) Monti, D.; Venanzi, M.; Mancini, G.; Di Natalec, C.; Paolesse, R. *Chem. Commun.* **2005**, 2471–2473. (f) Mizuno, Y.; Aida, T. *Chem. Commun.* **2003**, 20–21.

(9) (a) Paolesse, R.; Monti, D.; La Monica, L.; Venanzi, M.; Froiio, A.; Nardis, S.; Di Natale, C.; Martinelli, E.; D'Amico, A. *Chem.—Eur. J.* **2002**, *8*, 2476–2483. (b) Shoji, Y.; Tashiro, K.; Aida, T. *Chirality* **2008**, *20*, 420–424. (c) Hoeben, F. J. M.; Wolffs, M.; Zhang, J.; De Feyter, S.; Leclère, P.; Schenning, A. P. H. J.; Meijer, E. W. *J. Am. Chem. Soc.* **2007**, *129*, 9819–9828. (d) Monti, D.; Venanzi, M.; Stefanelli, M.; Sorrenti, A.; Mancini, G.; Di Natale, C.; Paolesse, R. *J. Am. Chem. Soc.* **2007**, *129*, 6688–6689. (e) Solladié, N.; Aubert, N.; Gisselbrecht, J.-P.; Gross, M.; Sooambar, C.; Troiani, V. *Chirality* **2003**, *15*, S50–S56.

(10) (a) Hodgson, M. J.; Borovkov, V. V.; Inoue, Y.; Arnold, D. P. *J. Organomet. Chem.* **2006**, *691*, 2162–2170. (b) Matassa, R.; Carbone, M.; Lauceri, R.; Purrello, R.; Caminiti, R. *Adv. Mater.* **2007**, *19*, 3961–3967. (c) Balaz, M.; De Napoli, M.; Holmes, A. E.; Mammana, A.; Nakanishi, K.; Berova, N.; Purrello, R. *Angew. Chem., Int. Ed.* **2005**, *44*, 4006–4009. (d) Hou, J.-L.; Yi, H.-P.; Shao, X.-B.; Li, C.; Wu, Z.-Q.; Jiang, X.-K.; Wu, L.-Z.; Tung, C.-H.; Li, Z.-T. *Angew. Chem., Int. Ed.* **2006**, *45*, 796–800.

(11) (a) Onouchi, H.; Miyagawa, T.; Morino, K.; Yashima, E. *Angew. Chem., Int. Ed.* **2006**, *45*, 2381–2384. (b) Mammana, A.; De Napoli, M.; Laucerib, R.; Purrello, R. *Bioorg. Med. Chem.* **2005**, *13*, 5159–5163. (c) Mammana, A.; D'Urso, A.; Lauceri, R.; Purrello, R. *J. Am. Chem. Soc.* **2007**, *129*, 8062–8063. (d) Bellacchio, E.; Lauceri, R.; Gurrieri, S.; Scolaro, L. M.; Romeo, A.; Purrello, R. *J. Am. Chem. Soc.* **1998**, *120*, 12353–12354. (e) Purrello, R.; Raudino, A.; Scolaro, L. M.; Loisi, A.; Bellacchio, E.; Lauceri, R. *J. Phys. Chem. B* **2000**, *104*, 10900–10908. (f) Borovkov, V. V.; Lintuluoto, J. M.; Inoue, Y. *Org. Lett.* **2002**, *4*, 169–171. (g) Ishii, Y.; Onda, Y.; Kubo, Y. *Tetrahedron Lett.* **2006**, *47*, 8221–8225.

(12) (a) Proni, G.; Pescitelli, G.; Huang, X.; Nakanishi, K.; Berova, N. *J. Am. Chem. Soc.* **2003**, *125*, 12914–12927. (b) Koto, Y.; Ohno, T.; Yamanaka, J.-I.; Tokita, S.; Iida, T.; Ishimaru, Y. *J. Am. Chem. Soc.* **2001**, *123*, 12700–12701. (c) Kurtán, T.; Nesnas, N.; Koehn, F. E.; Li, Y.-O.; Nakanishi, K.; Berova, N. *J. Am. Chem. Soc.* **2001**, *123*, 5974–5982. (d) Lauceri, R.; Raudino, A.; Scolaro, L. M.; Micali, N.; Purrello, R. *J. Am. Chem. Soc.* **2002**, *124*, 894–895.

(13) (a) Ribó, J. M.; Crusats, J.; Sagués, F.; Claret, J.; Rubires, R. *Science* **2001**, *292*, 2063–2066. (b) Rubires, R.; Farrera, J.-A.; Ribó, J. M. *Chem.—Eur. J.* **2001**, *7*, 436–446. (c) Escudero, C.; Crusats, J.; Díez-Pérez, I.; El-Hachemi, Z.; Ribó, J. M. *Angew. Chem., Int. Ed.* **2006**, *45*, 8032–8035. (d) El-Hachemi, Z.; Arteaga, O.; Canillas, A.; Crusats, J.; Escudero, C.; Kuroda, R.; Harada, T.; Rosa, M.; Ribò, J. M. *Chem.—Eur. J.* **2008**, *14*, 6438–6443. (e) Yamaguchi, T.; Kimura, T.; Matsuda, H.; Aida, T. *Angew. Chem., Int. Ed.* **2004**, *43*, 6350–6355. (f) Tsuda, A.; Alam, M. A.; Harada, T.; Yamaguchi, T.; Ishii, N.; Aida, T. *Angew. Chem., Int. Ed.* **2007**, *46*, 8198–8202.

(14) (a) Zhang, Y.; Chen, P.; Liu, M. *Chem.—Eur. J.* **2008**, *14*, 1793–1803. (b) Wang, T.; Liu, M. *Soft Matter* **2008**, *4*, 775–783. (c) Chen, P.; Ma, X.; Duan, P.; Liu, M. *ChemPhysChem* **2006**, *7*, 2419–2423. (d) Zhang, L.; Liu, M. *J. Phys. Chem. B* **2003**, *107*, 2565–2569. (e) Zhai, X.; Zhang, L.; Liu, M. *J. Phys. Chem. B* **2004**, *108*, 7180–7185.

(15) (a) Borovkov, V. V.; Hembury, G. A.; Yamamoto, N.; Inoue, Y. *J. Phys. Chem. A* **2003**, *107*, 8677–8686. (b) Borovkov, V. V.; Hembury, G. A.; Inoue, Y. *J. Org. Chem.* **2005**, *70*, 8743–8754. (c) Borovkov, V. V.; Hembury, G. A.; Inoue, Y. *Angew. Chem., Int. Ed.* **2003**, *42*, 5310–5314. (d) Borovkov, V. V.; Harada, T.; Hembury, G. A.; Inoue, Y.; Kuroda, R. *Angew. Chem., Int. Ed.* **2003**, *42*, 1746–1749. (e) Lintuluoto, J. M.; Borovkov, V. V.; Inoue, Y. *J. Am. Chem. Soc.* **2002**, *124*, 13676–13677. (f) Borovkov, V. V.; Lintuluoto, J. M.; Sugiura, M.; Inoue, Y.; Kuroda, R. *J. Am. Chem. Soc.* **2002**, *124*, 11282–11283.

(16) (a) Spada, G. P. *Angew. Chem., Int. Ed.* **2008**, *47*, 636–638. (b) Amabilino, D. B. *Nat. Mater.* **2007**, *6*, 924–925.

(17) (a) Zhang, Y.; Li, M.; Yang, R.; Liu, F.; Li, K. *J. Phys. Chem. A* **2005**, *109*, 7442–7448. (b) Cheng, B.; Munro, O. Q.; Marques, H. M.; Scheidt, W. R. *J. Am. Chem. Soc.* **1997**, *119*, 10732–10742.

(18) (a) De Luca, G.; Romeo, A.; Scolaro, L. M. *J. Phys. Chem. B* **2006**, *110*, 7309–7315. (b) De Luca, G.; Romeo, A.; Scolaro, L. M. *J. Phys. Chem. B* **2006**, *110*, 7309–7315. (c) Choi, M. Y.; Pollard, J. A.; Webb, M. A.; McHale, J. L. *J. Am. Chem. Soc.* **2003**, *125*, 810–820. (d) De Luca, G.; Pollicino, G.; Romeo, A.; Scolaro, L. M. *Chem. Mater.* **2006**, *18*, 2005–2007.

(19) (a) De Luca, G.; Romeo, A.; Scolaro, L. M. *J. Phys. Chem. B* **2006**, *110*, 14135–14141. (b) De Luca, G.; Romeo, A.; Scolaro, L. M. *J. Phys. Chem. B* **2005**, *109*, 7149–7158. (c) Li, X.; Li, D.; Zeng, W.; Zou, G.; Chen, Z. *J. Phys. Chem. B* **2007**, *111*, 1502–1506. (d) Okada, S.; Segawa, H. *J. Am. Chem. Soc.* **2003**, *125*, 2792–2796.

(20) (a) Koti, A. S. R.; Periasamy, N. *Chem. Mater.* **2003**, *15*, 369–371. (b) Barber, D. C.; Freitag-Beeston, R. A.; Whitten, D. G. *J. Phys. Chem.* **1991**, *95*, 4074–4086. (c) Micali, N.; Romeo, A.; Lauceri, R.; Purrello, R.; Mallamace, F.; Scolaro, L. M. *J. Phys. Chem. B* **2000**, *104*, 9416–9420. (d) Akins, D. L.; Zhu, H.-R.; Guo, C. *J. Phys. Chem.* **1996**, *100*, 5420–5425.

(21) (a) Yuan, J.; Liu, M. H. *J. Am. Chem. Soc.* **2003**, *125*, 5051–5056. (b) Huang, X.; Li, C.; Jiang, S.; Wang, X.; Zhang, B.; Liu, M. *J. Am. Chem. Soc.* **2004**, *126*, 1322–1323. (c) Zhang, Y.; Chen, P.; Jiang, L.; Hu, W.; Liu, M. *J. Am. Chem. Soc.* **2009**, *131*, 2756–2757.

(22) The concentrations of HCl and other HX ($X = Br^-$, I^-, and NO_3^-) acids were diluted to 2.4 and 1.2 M, respectively, before used as the subphase, in order to make sure that H_2TPPDOMe could be fully diprotonated in each case. In fact, 2.4 M HBr, HI, or HNO_3

was also used as the subphase, and a result similar to that derived from the corresponding 1.2 M subphase was achieved.

(23) (a) Spitz, C.; Dahne, S.; Ouart, A.; Abraham, H. W. *J Phys. Chem. B* **2000**, *104*, 8664–8669. (b) Yao, P.; Wang, H.; Chen, P.; Zhan, X.; Kuang, X.; Zhu, D.; Liu, M. *Langmuir* **2009**, *25*, 6633–6636.

(24) (a) Weissbuch, I.; Baxter, P. N. W.; Cohen, S.; Cohen, H.; Kjaer, K.; Howes, P. B.; Als-Nielsen, J.; Hanan, G. S.; Schubert, U. S.; Lehn, J.-M.; Leiserowitz, L.; Lahav, M. *J. Am. Chem. Soc.* **1998**, *120*, 4850–4860. (b) Cai, J.; Liu, M.; Yu, G.; Liu, Y. *J. Mater. Chem.* **2001**, *11*, 1924–1927. (c) Gong, H.; Yin, M.; Liu, M. *Langmuir* **2003**, *19*, 8280–8286. (d) Gong, H.; Liu, M. *Langmuir* **2001**, *17*, 6228–6232. (e) Chen, P.; Chen, Z.; Liu, M. *Colloids Surf., A* **2008**, *313–314*, 666–669.

(25) (a) Balasubramanian, K. K.; Cammarata, V.; Wu, Q. *Langmuir* **1995**, *11*, 1658–1665. (b) Rubinger, C. P. L.; Moreira, R. L.; Cury, L. A.; Fontes, G. N.; Neves, B. R. A.; Meneguzzi, A.; Ferreira, C. A. *Appl. Surf. Sci.* **2006**, *253*, 543–548.

(26) (a) Kasha, M.; Rawls, H. R.; Ashraf El-Bayoumi, M. *Pure Appl. Chem.* **1965**, *11*, 371–392. (b) McRae, E. G.; Kasha, M. *J. Chem. Phys.* **1958**, *28*, 271–277.

(27) (a) van Esch, J. H.; Feiters, M. C.; Peters, A. M.; Nolte, R. J. M. *J. Phys. Chem.* **1994**, *98*, 5541–5551. (b) Kano, H.; Kobayashi, T. *J. Chem. Phys.* **2002**, *116*, 184–195.

(28) (a) Togashi, D. M.; Romão, R. I. S.; da Silva, A. M. G.; Sobral, A. J. F. N.; Costa, S. M. B. *Phys. Chem. Chem. Phys.* **2005**, *7*, 3874–3883. (b) Choudhury, B.; Weedon, A. C.; Bolton, J. R. *Langmuir* **1998**, *14*, 6192–6198. (c) Gust, D.; Moore, T. A.; Moore, A. L.; Luttrull, D. K.; DeGraziano, J. M.; Boldt, N. J.; Van der Auweraer, M.; De Schryver, F. C. *Langmuir* **1991**, *7*, 1483–1490. (d) Qian, D.-J.; Nakamura, C.; Miyake, J. *Langmuir* **2000**, *16*, 9615–9619.

(29) (a) Viswanathan, R.; Zasadzinski, J. A.; Schwartz, D. K. *Nature* **1994**, *368*, 440–443. (b) Yashima, E.; Maeda, K.; Okamoto, Y. *Nature* **1999**, *399*, 449–451.

(30) (a) Ohiro, A.; Okoshi, K.; Fujiki, M.; Kunitake, M.; Naito, M.; Hagihara, T. *Adv. Mater.* **2004**, *16*, 1645–1650. (b) Gillgren, H.; Stenstam, A.; Ardhammar, M.; Nordén, B.; Sparr, E.; Ulvenlund, S. *Langmuir* **2002**, *18*, 462–469.

(31) Rosa, A.; Ricciardi, G.; Baerends, E. J.; Romeo, A.; Scolaro, L. M. *J. Phys. Chem. A* **2003**, *107*, 11468–11482.

(32) (a) Chen, P.; Ma, X.; Liu, M. *Macromolecules* **2007**, *40*, 4780–4784. (b) Qiu, Y.; Chen, P.; Liu, M. *Langmuir* **2008**, *24*, 7200–7207.

(33) Kral, V.; Furuta, H.; Shreder, K.; Lynch, V.; Sessler, J. L. *J. Am. Chem. Soc.* **1996**, *118*, 1595–1607.

AM900399W